Modeling And Control Battery Aging in Energy Harvesting Systems

Roberto Valentini*†, Nga Dang*, Marco Levorato*, Eli Bozorgzadeh*
* The Donald Bren School of Information and Computer Science, UC Irvine, CA, US
† Dept. of Information Engineering, Computer Science and Mathematics, University of L'Aquila, IT
e-mail: {rvalent1, levorato, ngad, ebozorgz}@uci.edu

arXiv:1511.03495v2 [cs.SY] 23 Nov 2015

***Abstract*— Energy storage is a fundamental component for the development of sustainable and environment-aware technologies. One of the critical challenges that needs to be overcome is preserving the State of Health (SoH) in energy harvesting systems, where bursty arrival of energy and load may severely degrade the battery. Tools from Markov process and Dynamic Programming theory are becoming an increasingly popular choice to control dynamics of these systems due to their ability to seamlessly incorporate heterogeneous components and support a wide range of applications. Mapping aging rate measures to fit within the boundaries of these tools is non-trivial. In this paper, a framework for modeling and controlling the aging rate of batteries based on Markov process theory is presented. Numerical results illustrate the tradeoff between battery degradation and task completion delay enabled by the proposed framework.**

I. Introduction

Energy storage systems represent a promising solution for smooth and robust integration of renewable energy sources to tomorrow's smart grid. In local micro-grid systems, the integration of energy storage has been proposed not only as an effective way to buffer the high peaks of energy demand (load) to the grid, but also to smooth out the uncertainty and fluctuations which characterize renewable energy sources. Furthermore, energy storage solutions are also proposed for electrical vehicles to achieve higher energy efficiency [1], self-sustainable communication devices [2], and cyber physical systems powered by renewable energy sources [3].

Among various technologies for energy storage, rechargeable batteries such as lithium-ion batteries are the prominent energy storage solution thanks to their relatively low cost and ability to hold charge. The main drawback of this technology is the limited battery life time and power density. Batteries cannot be charged and discharged an unlimited number of times due to aging effect. Their State of Health (SoH) not only depends on charge/discharge cycle counts (battery lifetime), but are also depends on charge/discharge rate (power density). As a consequence, the aging effect in batteries is even more dominant when deployed in renewable energy systems. Harnessing energy *opportunistically* from renewable sources causes a dynamic fluctuation in the charge level which may significantly degrade their SoH. In such systems, if the battery aging effect is not limited, the effective capacity and energy density may rapidly deteriorate. This paper proposes a novel modeling and optimization framework to capture and control the aging rate of batteries in these critical systems.

A considerable research effort is undergoing to develop models for the degradation of the SoH of batteries over time. This is motivated by the possibility to design Energy Harvesting Systems (EHSs) relying on batteries with extended lifetime. In [4], the author proposes a degradation model for lithium batteries, which is used in [5] and [6] to optimize battery usage under aging constraints. These works demonstrate that the SoH degradation rate can be quantified as a function of the battery usage in terms of the average energy amount stored in the battery, named as average SoC and its standard deviation over a time window.

Based on these works, in this paper we present a novel framework for the modeling and control of the SoH of batteries in EHSs. Different from prior work, the proposed framework models the temporal evolution of the system as a Stochastic Finite State Machine (SFSM) [7]. This modeling rationale is becoming increasingly popular in a variety of Smart Grid related applications [8]–[15]. For instance in [8], a SFMS model capturing the dynamics of appliance activation and energy scheduling for residential demand response is presented. To minimize the weighted sum of the average financial cost of operations and appliance activation delay, the authors proposed a reinforcement learning approach. In [14], a Markov chain framework is proposed to find the optimal storage control policy for smarts power grids. In [2], the optimal utility scheduling for energy harvesting networks is analyzed. However, in these works, battery aging was not considered. The popularity of frameworks based on a SFSM/Markovian representation over other options comes from the inherent simplicity of the model, which captures key dependencies in the temporal evolution of the system, as well as interdependencies in the evolution (*e.g.*, activation, de-activation) of individual components. This representation also enables the use of a wide range of well studied analysis and optimization tools such as dynamic programming [16] and hidden Markov models [17].

Herein, we develop a model and control framework that explicitly includes battery aging metrics in the optimization problem determining the behavior of the system. In [18], he authors propose a stochastic Markov chain optimization approach, where the age of the battery is explicitly included in the systems state. However, the temporal scale of battery degradation is much larger than systems' time scale operations. As a consequence, the approach in [18] results in a coarse approximation of battery aging. In this paper, we take a different approach by including metrics controlling the *rate of aging* in the optimization problem.

In order to make the scope of the proposed methodology as broad as possible, we consider a general EHS. The proposed formulation and metrics can be directly plugged into dynamic programming frameworks [16]. The considered system allows to explore the tension between the minimization of the waiting time of energy tasks generated, and stored, by the load module, and the need to avoid excessive SoC fluctuations. In particular, we show that SoH degradation can be reduced at the cost of a

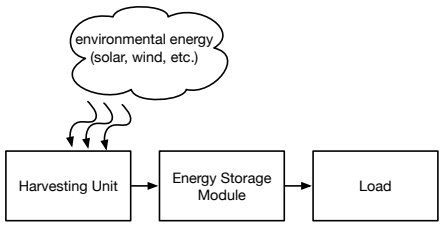

Fig. 1. Energy Harvesting System considered in this paper.

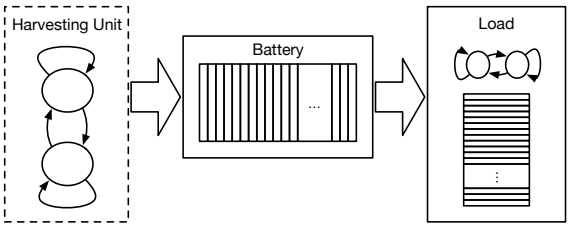

Fig. 2. System Model.

higher task completion delay. However, admitting this increased system delay may be necessary to avoid dramatic long-term system performance degradation in some cases.

The rest of this paper is organized as follows. In Section II, we introduce the SFSM system model. The battery aging modeling and definition of the associated cost functions are provided in Sections III. The optimization framework is described in Section IV. In Section V numerical results are presented. Section VI concludes the paper.

II. System Model

We consider a general system composed of three main modules (see Fig. 1): the energy harvesting unit, the energy storage module, and the load module. The energy harvesting unit collects and converts energy from the environment to power the downstream modules. The energy storage device stores the energy acquired by the energy harvesting module, and interfaces with the load module, which models the arrival and queueing of energy requests from the application.

The system depicted in Fig. 1 is instantiated as a SFSM with Markovian transitions. Slotted time is assumed, where the index $\tau \in \mathbb{Z}^+$ indicates the time interval $[\tau\Delta T, \tau\Delta T + \Delta T)$, where ΔT is the slot duration. The overall FSM results from the composition of sub-FSMs associated with the individual components (energy harvesting, battery and load).

Fig. 2 illustrates the components of the system interpreted as FSMs. The arrival of energy at the harvesting unit is modeled as the Markov process $\mathbf{H}=\{H_0, H_1, \ldots\}$, where $H_\tau \in \mathcal{H}$ is the harvesting state at time τ, and $\mathcal{H}$ is the finite state space. Define E_τ as the number of energy units entering the system at time τ. Each state h in $\mathcal{H}$ is associated with a distribution $f_h(e)$, where

$$f_h(e)=\mathcal{P}(E_\tau=e|H_\tau=h). \tag{1}$$

The temporal evolution of the harvesting process is governed by the transition probabilities

$$p_{\gamma_h}(h'|h)=\mathcal{P}(H_{\tau+1}=h'|H_\tau=h,\gamma_h), \tag{2}$$

where γ_h is a parameter set. Note that the sequence of energy unit arrivals $\{E_0, E_1, \ldots\}$ is not a Markov process.

The battery is modeled as an "energy buffer" with nominal capacity $Q_{\max}$. The SoC is uniformly quantized with quantization step ΔQ. Thus, the charge level at slot τ, Q_τ, takes values in the finite set $\mathcal{Q}=\{0, \ldots, Q_{\max}\}$. The temporal dynamics of the SoC are determined by the update equation

$$Q_{\tau+1}=\max\{Q_\tau - A_\tau, 0\} + E_\tau, \tag{3}$$

where A_τ indicates the number of energy units used in slot τ. As clarified later, $A_\tau \in \mathcal{A}=\{0\} \cup \{A_{\min}, \ldots, A_{\max}\}$ is the "action" variable to be optimized. We assume that any combination of variables in the right hand side of Eq. (3) generates an element in $\mathcal{Q}$. Alternatively, $\max\{Q_\tau - A_\tau, 0\} + E_\tau$ can be mapped to the closest element in $\mathcal{Q}$.

The load is modeled as a sequence of energy tasks to be completed. The energy tasks are stored in a finite buffer, and their arrival is governed by a Markov process similar to that of energy arrival. Then, we define the Markov process $\mathbf{L}=\{L_0, L_1, \ldots\}$, where $L_\tau \in \mathcal{L}$ is the state of the load in slot τ and $\mathcal{L}$ is the load state space. The temporal evolution of the load state is determined by the transition probabilities

$$p_{\gamma_l}(l'|l)=\mathcal{P}(L_{\tau+1}=l'|L_\tau=l,\gamma_l), \tag{4}$$

where γ_l is a parameter set. Each state $l \in \mathcal{L}$ is associated with the generation of an energy task whose completion necessitates a number of energy units U determined by the distribution $f_l(U)$, where

$$f_l(u)=\mathcal{P}(U_\tau=u|L_\tau=l), \tag{5}$$

and U_τ is the number of energy units requested at time τ. The amount of energy units that has been requested, and not yet deployed, in slot τ is equal to $W_\tau \in \mathcal{W}=\{1, \ldots, W_{\max}\}$. The update rule of W_τ, then, is

$$W_{\tau+1}=\max(0, W_\tau - A_\tau) + U_\tau. \tag{6}$$

Analogously to the update of the battery SoC, we build the system so that any combination of variables in the right hand side of Eq. (6) generates an element in $\mathcal{W}$. The above transition probabilities and update rules can be used to define the transition probabilities of the three modules as a function of the action distribution as described later in this paper.

We remark that the general FSM defined above can be adapted to capture the dynamics of systems with a higher complexity without the need for any major modification of the battery aging metrics and framework. For instance, the integration in the model of deadlines for the completion of energy tasks necessitates the inclusion of time counters in the state space representation of the load module.

III. Battery Aging and Cost Functions

Due to battery usage, the maximum charge level $Q_{\max}$ of the battery decays over time. Denote with $Q_{\max}(t)$ the battery capacity at time t, then $Q_{\max}(t) \leq Q_{\max}(t-1)$, and $Q_{\max}(0)=Q_{\max}$. We adopt the battery degradation model proposed in [4] for continuous time systems, in which the rate of SoH degradation over a time interval $[0, T]$, is a function of the average SoC,

standard deviation of the SoC and the effective number of cycles, defined as

$$SoC_{avg} = \frac{1}{T}\int_0^T SoC(t)dt, \tag{7}$$

$$SoC_{dev} = 2\sqrt{\frac{3}{T}\int_0^T (SoC(t) - SoC_{avg})^2 dt}, \tag{8}$$

$$N_{\text{cyc}} = \frac{1}{2Q_{\text{norm}}}\int_0^T \mid I(t) \mid dt, \tag{9}$$

respectively, where $I(t)$ is the charging/discharging current of the battery. Based on the above metrics, the battery degradation $D_{\eta,T}{=}f(SoC_{avg}, Soc_{dev}, N_{\text{cyc}})$ in the target period, then, is computed as follows

$$D_{\eta,T} = D'\ C\ e^{D(SoC_{avg}-0.5)}, \tag{10}$$

$$D'{=}A\ N_{\text{cyc}}\ e^{(SoC_{dev}-1)B} + 0.2\frac{T}{T_{life}}, \tag{11}$$

where A,B,C,D and T_{life} are constants associated with physical properties of the battery [4]. However, different aging models can be easily incorporated in the optimization framework described in the next section. For instance, in [19] the authors provide an empirical demonstration that the variable N_{cyc} has not a significant effect. In our framework, such modification only requires the removal of a constraint in the optimization problem.

Thus, battery aging exponentially increases with SoC_{avg} and SoC_{std}, while linearly increases with N_{cyc}. Hence, in order to avoid high SoH degradation, the system needs to operate in low-charging levels and avoid SoC fluctuations with respect to the average SoC. We remark that the time scale of battery aging is much larger compared to the time scale of the system's operations. Thus, rather than including the SoH in the state representation, our framework aims at minimizing the *aging rate* over long time periods.

In order to apply dynamic programming techniques, the metrics defined in Eqs. (7), (8), and (9) need to be transformed into time averages of additive cost functions mapped onto the state-action space of the system. To obtain a representation with manageable complexity, this should be achieved by adding the smallest possible number of states to the state space. For the system described in Sec. II, the discretized version of the metrics is

$$Q_\mu = \frac{1}{T}\sum_{\tau=0}^{T} Q_\tau, \tag{12}$$

$$Q_\sigma^2 = \frac{1}{T}\sum_{i=0}^{T} (Q_\tau - Q_\mu)^2, \tag{13}$$

$$N_{\text{cyc}} = \frac{1}{2Q_{\text{nom}}}\sum_{\tau=0}^{T} |A_\tau| + |E_\tau|, \tag{14}$$

where T is the number of considered slots.

While the metrics in Eqs. (12) and (14) find a direct transposition in the desired form, the metric in Eq. (13) requires a priori knowledge of the average SoC. Unfortunately, the average SoC is itself a function of the control, and Q_σ^2 does not find a direct representation compatible with dynamic programming cost functions. To overcome this issue, we define a set of metrics

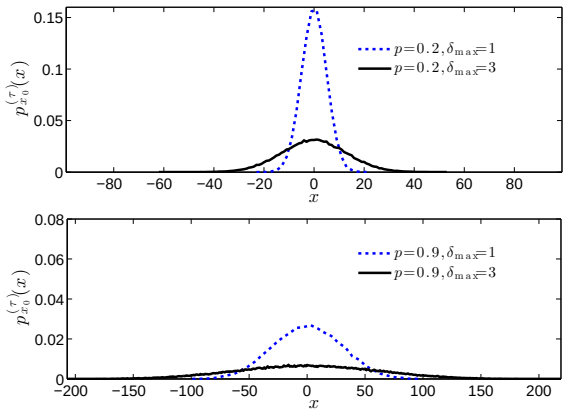

Fig. 3. Limiting distribution of the charge level $p_{x_0}^{(\tau)}(x)$ as a function of deviation from mean charge, for different values of the persistence parameter p and the maximum step amplitude $\delta_{\max}$

whose minimization corresponds to the minimization of Q_σ^2. Define, then,

$$\Delta = \frac{1}{T}\sum_{\tau=0}^{T} |\Delta_\tau|, \tag{15}$$

$$V = \frac{1}{T-1}\sum_{\tau=1}^{T} \mathbb{1}(\text{sgn}(\Delta_\tau){=}\text{sgn}(\Delta_{\tau-1})), \tag{16}$$

where $\Delta_\tau{=}Q_\tau - Q_{\tau-1}$, $\mathbb{1}(\cdot)$ the indicator function and $\text{sgn}(\cdot)$ is the sign function. Note that Δ, represents the average amplitude of battery charge/discharge phases, while V measures the average duration of a charge phase until battery starts discharging and conversely.

It can be proved that bounding Δ and V is equivalent to bounding the SoC standard deviation. Due to space limitations, we only provide a sketch of the proof. The SoC process can be modeled as a one-dimensional *persistent random walk* [20], for which the next step is taken in the same direction of the previous with probability p. Furthermore, consider a step amplitude δ, uniformly distributed in $[1, \delta_{\max}]$. The τ-step distribution conditioned on the initial state $Q_0{=}x_0$, that is, $p_{x_0}^{(\tau)}(x){=}\mathcal{P}(Q_\tau{=}x|Q_0{=}x_0)$, converges to a Gaussian distribution when τ tends to infinity and the continuos limit is considered. The second moment of the limiting distribution, $\sigma^2{=}\bar{\delta}\tau p/(1{-}p)$, is a function of p and the average step amplitude $\bar{\delta}$. Thus, by controlling the persistence p and $\bar{\delta}$, which in our model corresponds to the control of V and Δ respectively, the standard deviation of the process can be bounded. Fig. 3 illustrates these interdependency between the cost metrics and the SoC variance.

IV. Optimization Framework

We formulate an optimization problem aiming at minimizing the completion delay of the energy tasks with a bounded aging rate of the battery. Following the approach in [8], we define the auxiliary variable

$$Y_{\tau+1} = \theta\ Y_\tau + (1{-}\theta)\ W_\tau, \tag{17}$$

with $0{<}\theta{<}1$. Y_τ exponentially smooths the task energy backlog and, thus, represents an indicator of the average waiting time until all pending tasks are accomplished. When $\theta{=}0$, then

$Y_{\tau+1}{=}W_\tau$ and Y_τ measures the instantaneous load queue length. Note that Y_τ is a real valued variable, thus, we discretize the auxiliary variable to maintain model tractability, assuming that it takes values on a discrete finite set $\mathcal{Y}$.

The optimization problem can be formulated as a Constrained Markov Decision Process (CMDP) [21] aiming at the minimization of the objective function

$$C = \lim_{T\to\infty} \frac{1}{T} E\left[\sum_{\tau=0}^{T} f(Y_\tau)\right], \tag{18}$$

where $f(\cdot)$ is a convex function, under constraints on the following time averages

$$Q_\mu = \lim_{T\to\infty} \frac{1}{T} E\left[\sum_{\tau=0}^{T} Q_\tau\right], \tag{19}$$

$$N_{\text{cyc}} = \lim_{T\to\infty} \frac{1}{T} E\left[\sum_{\tau=0}^{T} |A_\tau| + |E_\tau|\right], \tag{20}$$

$$\Delta = \lim_{T\to\infty} \frac{1}{T} E\left[\sum_{\tau=0}^{T} |\Delta_\tau|\right], \tag{21}$$

$$V = \lim_{T\to\infty} \frac{1}{T} E\left[\sum_{\tau=0}^{T} g(\Lambda_\tau)\right]. \tag{22}$$

The definition of the cost function in Eq. (22) necessitates the inclusion in the model of the logical variable Λ_τ, where $\Lambda_\tau{=}1$ if $\Delta_\tau{>}0$, corresponding to instantaneous (i.e., slot-by-slot) charging, and $\Lambda_\tau{=}0$ if $\Delta_\tau{>}0$, corresponding to instantaneous discharging. By introducing a function $g(\cdot)$, such that $g(\Lambda_\tau){=}1$, if $\Lambda_\tau{=}\Lambda_{\tau-1}$, and $g(\Lambda_\tau){=}0$ otherwise, we measure the duration of charging and discharging phases.

Note that the objective function and constraints are defined as time averages over an infinite time horizon. This formulation originates from the assumption that battery aging occurs at a time scale much larger than that of the system's operations.

The overall system state Z_τ at time τ is defined to be the composition of all *physical* sub-FSMs (i.e., harvesting, charge level, load), and the auxiliary variable Y_τ and the flag Λ_τ, which are *logical* sub-FSMs required to measure the average tasks' completion delay and battery degradation. In particular:

$$Z_\tau = (H_\tau, Q_\tau, W_\tau, Y_\tau, L_\tau, \Lambda_\tau), \tag{23}$$

with $Z_\tau{\in}\mathcal{Z}{=}\mathcal{H}{\times}\mathcal{Q}{\times}\mathcal{W}{\times}\mathcal{Y}{\times}\mathcal{L}{\times}\{0,1\}$. The transition probabilities are defined as $p(z'|z,a){=}\mathcal{P}(Z_\tau{=}z'|Z_\tau{=}z, A_\tau{=}a)$, whit $z', z{\in}\mathcal{Z}$, $a{\in}\mathcal{A}$ and can be factorized as in Eq. (24), given conditional independence between the various system components.

Without any loss of optimality, we constrain our search within the class of past-independent randomized policies $\mu\colon \mathcal{Z}{\times}\mathcal{A}{\to}[0,1]$ [21], where $\mu(a|z){=}\mathcal{P}(A_\tau{=}a|Z_\tau{=}z)$ is the probability of choosing action a given that the system is in state z. Thus, the long-run objective in (18) can be redefined as a function of states and actions:

$$C_\mu = \sum_{z\in\mathcal{Z}} \sum_{a\in\mathcal{A}} \pi_\mu(z,a) c(z,a) \tag{25}$$

where $\pi_\mu(z,a){=}\mathcal{P}_\mu(Z_\tau{=}z, A_\tau{=}a)$ is the stationary joint distribution of states and actions, $E_\mu[\cdot]$ is the expectation operator under policy μ and $c(z,a)$ is the value of the objective function incurring in state z under action a.

Similar arguments hold for the time averages in Eqs. (19), (20), (21), and (22), that can be mapped into functions of states and actions, $d^k\colon \mathcal{Z}{\times}\mathcal{A}{\to}\mathbb{R}$, with $k{=}\{1,2,3,4\}$. Each long-run average cost can be expressed as

$$D^k_\mu = \sum_{z\in\mathcal{Z}} \sum_{a\in\mathcal{A}} \pi_\mu(z,a) d^k(z,a). \tag{26}$$

Due to space constraints, we do not include a detailed description of the intuitive mapping between time averages and state-action functions.

The optimization problem can be formulated as

$$\begin{aligned} \underset{\mu}{\text{minimize}} \quad & C_\mu \\ \text{s.t.} \quad & D^k_\mu \le \hat{c}^k,\ k = 1,\dots,4. \end{aligned} \tag{27}$$

where $\hat{c}^k$ is the upper bound for average cost of type k. This optimization problem is equivalent to the following linear program [21],

$$\underset{\mu}{\text{minimize}} \quad \sum_{z\in\mathcal{Z}} \sum_{a\in\mathcal{A}} x_{za} c(z,a) \tag{28}$$

$$\text{s.t.} \quad \sum_{a\in\mathcal{A}} x_{za} - \sum_{z\in\mathcal{Z}} \sum_{a\in\mathcal{A}} x_{za} p(z'|z,a) = 0 \tag{29}$$

$$\sum_{z\in\mathcal{Z}} \sum_{a\in\mathcal{A}} x_{za} d^k(z,a) \le \hat{c}^k,\ k = 1,\dots,4 \tag{30}$$

$$\sum_{z\in\mathcal{Z}} \sum_{a\in\mathcal{A}} x_{za} = 1 \tag{31}$$

$$x_{za} \ge 0, \tag{32}$$

where the decision variables $x_{za}{=}\pi(z,a)$ are the steady state joint distributions of the states and actions. Then, the optimal stationary policy $\mu^\star$ can be computed as

$$\mu^\star(a|z) = \frac{x_{za}}{\sum_{a\in\mathcal{A}} x_{za}}. \tag{33}$$

V. Numerical Results

In this section, we compare the performance of the aging-aware and age-unaware policies, and examine the tradeoff between the waiting time of backlogged energy tasks and SoH degradation. In particular, the resulting long-run average objective function and SoH degradation are analyzed for the constrained problem in Eq. (27), and the associated unconstrained version.

We consider binary Markovian input processes **H** and **L**, that is, $H_\tau{\in}\{0,1\}$ and $L_\tau{\in}\{0,1\}$. Furthermore, we assume that when $H_\tau{=}0$, no energy units arrive in the system, otherwise only one energy unit is generated with probability one. This corresponds to set $\mathcal{P}(E_\tau{=}e|H_\tau{=}0){=}0$ and $\mathcal{P}(E_\tau{=}1|H_\tau{=}1){=}1$. A similar model is used for the task arrival process.

The transition probabilities for the input processes are defined by the parameter set $\gamma_i{=}(\phi_i, b_i)$, where ϕ_i and b_i are the arrival rate and the average length of sequences of state "1" respectively. The index $i{=}h,l$, corresponds to the harvesting process (h) or the task arrival process (l). For the considered arrival model, the

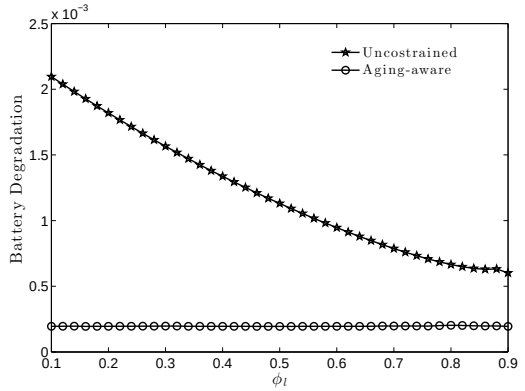

Fig. 4. Battery degradation as a function of tasks arrival rate ϕ_l

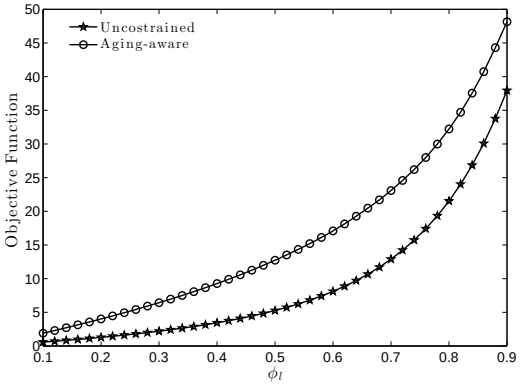

Fig. 6. Objective function over tasks arrival rate ϕ_l

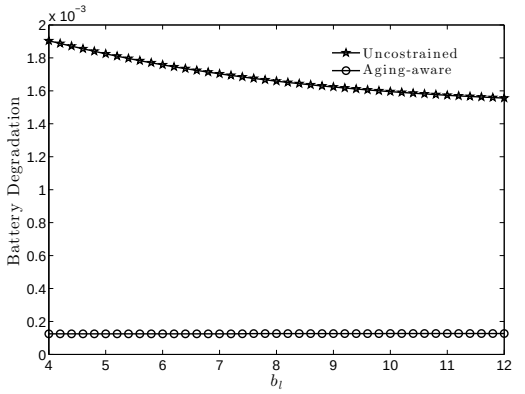

Fig. 5. Battery degradation as a function of task arrival process burstiness b_l

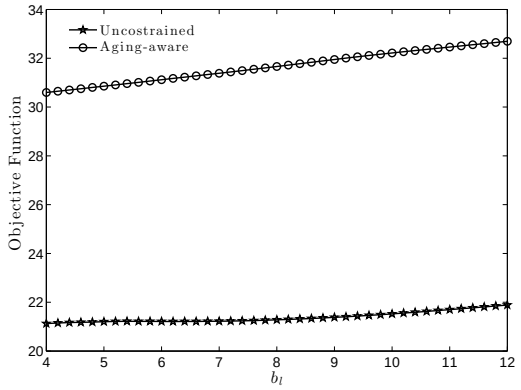

Fig. 7. Objective function over task arrival process burstiness b_l

arrival rate corresponds to the steady state probability of state "1". Consequently, we have

$$p_{\gamma_i}(0|1) = \frac{1}{b_i}, \quad p_{\gamma_i}(1|0) = \frac{\phi_i}{b_i(1-\phi_i)}. \tag{34}$$

In the numerical results, we set ϕ_h=0.9 and b_h=10, meaning that the harvesting module frequently injects long bursts of energy into the system. The load arrival process has parameters ϕ_l=0.8 and b_l=12. SoH degradation is computed based on the parameters of the battery cell for Plug-in Hybrid Electric Veichles (PHEVs) considered in [4], where the corresponding values for constants A,B,C,D and T_{life} are provided. For computational purposes we set $Q_{\max}$=$W_{\max}$=8 and we assume binary action space $\mathcal{A}$=$\{0,1\}$. Thus, the load can only remains "idle" or draws at most one energy unit from the battery that is sufficient for the completion of a task. Finally, in order to guarantee strict convexity of the objective function, we set $f(Y_\tau)$=Y_τ^2 and we choose θ=0.1.

As shown in Fig. 4, the aging-aware control policy guarantees low and almost constant degradation rate for different values of ϕ_l and b_l=10 with respect to the unconstrained policy. Note that when the aging constraints are removed, degradation rate decreases as the tasks arrival rate increases. This can be justified noting that, for fixed harvesting conditions, high values of ϕ_l correspond to frequent task arrivals, and consequently, frequent energy usage, leading to small values of SoC_{avg}, thus inducing a lower degradation rate.

Fig. 5 shows the aging rate as a function of the burstiness of the task arrival process b_l. Degradation is less sensitive to b_l variations and slightly decreases as the load burstiness increases. Also in this case, the battery aging-aware approach guarantees very low and almost constant degradation rate.

Bounding the energy degradation by setting the constraints defined before generates a larger task-completion time. This is shown in Fig. 6 where, for every value of the tasks arrival rate, the aging-aware policy always results in higher delay. Note also that, as expected, the average waiting time increases as the load arrival rate increases.

For completeness, in Fig. 7 we also show the long-run average task completion delay as a function of the load burstiness b_l. We found that delay is less sensitive to burstiness of the load. However, the average delay induced by the constrained policy is still higher than that resulting from the unconstrained policy.

In order to provide some intuition on the structure of the

$$p(z'|z,a) = p_{\gamma_h}(h'|h)\ p(q'|q,a)\ p(w'|w,a)\ p(y'|y,w)\ p_{\gamma_l}(l'|l)\ p(\lambda'|q',q)$$
$$h,h' \in \mathcal{H},\ q,q' \in \mathcal{Q},\ w,w' \in \mathcal{W},\ y,y' \in \mathcal{Y},\ l,l' \in \mathcal{L},\ \lambda' \in \{0,1\}. \tag{24}$$

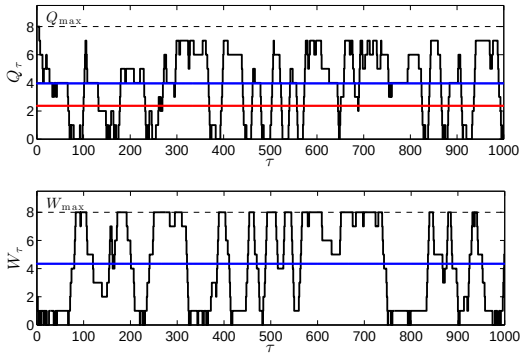

Fig. 8. Trace simulation under unconstrained policy. Heavy load, $\phi_l = 0.8$, $b_l = 12$. The blue line represents average and the red line represents standard deviation

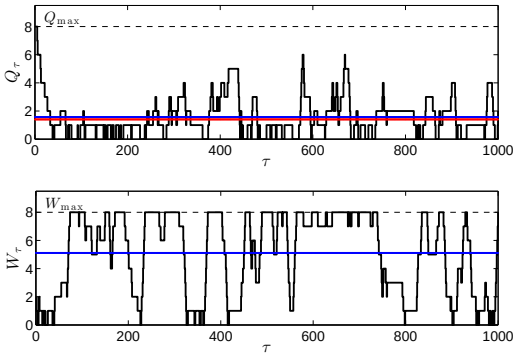

Fig. 9. Trace simulation under aging-aware policy. Heavy load, $\phi_l = 0.8$, $b_l = 12$. The blue and red lines represent average and standard deviation, respectively.

control policies, we ran 1000 samples Monte Carlo simulations both for the constrained and the unconstrained optimal policy. The resulting charge level and task backlog traces are depicted in Fig. 8 (unconstrained policy) and Fig. 9 (aging-aware policy). The load buffer is assumed to operate under "heavy load" conditions, in particular we set ϕ_l=0.8 and b_l=12. As expected, the unconstrained policy results in a high number of charge/discharge cycles characterized by frequent and larger fluctuations around the mean value, whereas the aging-aware policy forces the battery to operate in a low SoC_{avg} regime characterized by smaller fluctuations around the mean, which is in turn kept bounded. Consequently the SoC profile results smoother. This guarantees a low SoH degradation rate, thus prolonging battery lifetime and increasing system reliability. However, the aging-aware policy results in higher average backlogs with buffer saturation condition for 35.1% of the time, against 28.2% of the unconstrained policy.

VI. Conclusions

In this paper, we presented a stochastic modeling and control framework for battery aging in EHS based on SFSM. Inspired by an existing battery degradation model, we introduced performance and aging measures that can be directly plugged into a CMDP in form of average cost functions. A linear program was proposed to solve the optimization problem, whose solution is the optimal randomized policy minimizing the average waiting time of energy tasks stored in a system queue with bounded degradation rate. Numerical results were provided to illustrate the tradeoff between system performance and battery degradation.

References

[1] J. Dixon, "Energy storage for electric vehicles," in *IEEE International Conference on Industrial Technology (ICIT)*. IEEE, 2010, pp. 20–26.

[2] L. Huang and M. Neely, "Utility optimal scheduling in energy-harvesting networks," *IEEE/ACM Transactions on Networking*, vol. 21, no. 4, pp. 1117–1130, Aug 2013.

[3] N. Dang, H. Tajik, N. Dutt, N. Venkatasubramanian, and E. Bozorgzadeh, "Orchestrated application quality and energy storage management in solar-powered embedded systems," in *16th International Symposium on Quality Electronic Design (ISQED)*. IEEE, 2015, pp. 227–233.

[4] A. Millner, "Modeling lithium ion battery degradation in electric vehicles," in *IEEE Conference on Innovative Technologies for an Efficient and Reliable Electricity Supply (CITRES)*, 2010, pp. 349–356.

[5] Q. Xie, X. Lin, Y. Wang, M. Pedram, D. Shin, and N. Chang, "State of health aware charge management in hybrid electrical energy storage systems," in *Design, Automation Test in Europe Conference Exhibition (DATE)*, 2012, pp. 1060–1065.

[6] Y. Wang, X. Lin, Q. Xie, N. Chang, and M. Pedram, "Minimizing state-of-health degradation in hybrid electrical energy storage systems with arbitrary source and load profiles," in *Design, Automation and Test in Europe Conference and Exhibition (DATE)*, 2014, pp. 1–4.

[7] H. M. Taylor and S. Karlin, *An introduction to stochastic modeling*. John Wiley & Sons, 1994.

[8] D. O'Neill, M. Levorato, A. Goldsmith, and U. Mitra, "Residential demand response using reinforcement learning," in *First IEEE International Conference on Smart Grid Communications (SmartGridComm)*, 2010, pp. 409–414.

[9] K. Turitsyn, S. Backhaus, M. Ananyev, and M. M. Chertkov, "Smart finite state devices: A modeling framework for demand response technologies," in *50th IEEE Conference on Decision and Control and European Control Conference*, Dec 2011, pp. 7–14.

[10] M. Levorato and U. Mitra, "Fast anomaly detection in smartgrids via sparse approximation theory," in *IEEE 7th Sensor Array and Multichannel Signal Processing Workshop (SAM)*, 2012, pp. 5–8.

[11] B. Jiang and Y. Fei, "Dynamic residential demand response and distributed generation management in smart microgrid with hierarchical agents," *Energy Procedia*, vol. 12, pp. 76–90, 2011.

[12] H. Tischer and G. G. Verbic, "Towards a smart home energy management system-a dynamic programming approach," in *IEEE PES Innovative Smart Grid Technologies Asia (ISGT)*, 2011, pp. 1–7.

[13] M. Goonewardena and L. B. Le, "Charging of electric vehicles utilizing random wind: A stochastic optimization approach," in *2012 IEEE Globecom Workshops*. IEEE, 2012, pp. 1520–1525.

[14] I. Koutsopoulos, V. Hatzi, and L. Tassiulas, "Optimal energy storage control policies for the smart power grid," in *IEEE International Conference on Smart Grid Communications (SmartGridComm),*, 2011, pp. 475–480.

[15] M. Levorato, N. Ahmed, and Y. Zhang, "Consumer in-the-loop: Consumers as part of residential smart energy systems," in *IEEE International Conference on Smart Grid Communications (SmartGridComm)*, 2014, pp. 758–763.

[16] D. P. Bertsekas, *Dynamic programming and optimal control*. Athena Scientific Belmont, MA, 1995, vol. 1, no. 2.

[17] R. J. Elliott, L. Aggoun, and J. B. Moore, *Hidden Markov Models*. Springer, 1995.

[18] N. Michelusi, L. Badia, R. Carli, L. Corradini, and M. Zorzi, "Energy management policies for harvesting-based wireless sensor devices with battery degradation," *IEEE Transactions on Communications*, vol. 61, no. 12, pp. 4934–4947, December 2013.

[19] L. Lam and P. Bauer, "Practical capacity fading model for li-ion battery cells in electric vehicles," *Power Electronics, IEEE Transactions on*, vol. 28, no. 12, pp. 5910–5918, 2013.

[20] E. Renshaw and R. Henderson, "The correlated random walk," *Journal of Applied Probability*, pp. 403–414, 1981.

[21] K. Ross, "Randomized and past-dependent policies for markov decision processes with multiple constraints," *Operations Research*, vol. 37, no. 3, pp. 474–477, 1989.